Contents lists available at Science-Gate

International Journal of Advanced and Applied Sciences

Journal homepage: http://www.science-gate.com/IJAAS.html

Implementation and analysis of symmetrical signals in the sequency domain

Dur-e-Jabeen [1,*], M. Ghazanfar Monir [2], M. Rafiullah [3], Faiza Waqqas [1], Habib Shaukat [1]

[1]Department of Electronic Engineering, Sir Syed University of Engineering and Technology, Karachi, Pakistan
[2]Department of Electronic Engineering, Muhammad Ali Jinnah University, Karachi, Pakistan
[3]Department of Mathematics, COMSATS University Islamabad, Lahore, Pakistan

ARTICLE INFO

Article history:
Received 23 October 2022
Received in revised form
23 February 2023
Accepted 29 March 2023

Keywords:
Symmetry properties
Real values
Imaginary values
Complex axis
Phasor rotations

ABSTRACT

Every transform has unique attributes and traits that are crucial to reducing computing costs and offering simple solutions. Many different frequency domain transformations, for instance, have properties that can be used in a variety of signal processing applications and analyses. Some of the Complex Hadamard Transform's variants' sequencies can be compared to those of the Discrete Fourier Transforms. It is proven the characteristics of the Conjugate Symmetric Sequency-Ordered Complex Hadamard Transform symmetry. These qualities are crucial for signal analysis and image processing. Due to duplicate spectra across the origin, it reduces computational complexity, makes an analytical analysis for symmetric signals simpler, and needs less storage. Its analysis shows that the Discrete Fourier Transform and this Complex Hadamard Transform version exhibit similar symmetry tendencies. By using elementary signals in the time domain to connect the positive and negative sequencies with their associated phasor conceptions, sequency domain spectra are used to highlight these properties. As a result of image representation, relative spectra are represented in related domains. Transform can be used to extract and analyze various aspects from a wide range of medical images.

1. Introduction

Applications for signal processing frequently use discrete orthogonal transforms (DOTs) (Mahmmod et al., 2018; Asli and Flusser, 2017; Bahrami and Naderi, 2014; Tian et al., 2018; Shukla and Sharma, 2018; Usman et al., 2020). Researchers have become interested in the Complex Hadamard Transform (CHT) DOT, to investigate the various field of study by applying the applications of signal and image processing. CHT is the generalized version of the Walsh Hadamard Transform due to its simplicity of use and ability to generate the transformation matrix (WHT). There are numerous CHT variations have been generated in Rahardja and Falkowski (1999) and Aung (2009). Before any CHT variants can replace the Discrete Fourier Transform (DFT) in signal processing applications, need to validate the designed features by applying various (Dur-e-Jabeen et al., 2016; Dur-e-Jabeen and Monir, 2016; Aung et al., 2009). CHT matrix values lie on the unit circle (Aung et al., 2009; Aung, 2009). Similar to the DFT in a frequency domain, it operates in the Sequency Domain (SD).

Proakis (2007) expressed and illustrates the Fourier series as a set of discrete and periodic functions, which is the sum of sine and cosine functions at various frequency coefficients. If the signal is aperiodic, it can be represented mathematically using the Fourier Transform (FT) as the sum of sinusoidal functions. In real-world situations, FT is preferable to the Fourier series. This paper is focused on the Conjugate symmetric Sequency Ordered Complex Hadamard Transform (CS-SCHT) (Aung et al., 2009), whose transformation matrix is unitary, orthogonal, and possesses conjugate symmetric in nature as DFT, is the subject of this study. It has symmetry elements or properties in SD that are comparable to the symmetry elements in the frequency domain (FD) found in DFT (Rehman and Mehmood, 2018). In order to approximate square waveforms with low and high values for the DFT, CS-SCHT (Aung et al., 2009) calculated sine and cosine waveforms. As a result, the CS-SCHT

* Corresponding Author.
Email Address: durejabeen@hotmail.com (Dur-e-Jabeen)
https://doi.org/10.21833/ijaas.2023.05.023
Corresponding author's ORCID profile:
https://orcid.org/0000-0002-6743-2911

formulation offers the sum of square basis functions multiplied by their coefficients at various sequencies. According to Fig. 1a, the CS-SCHT offers an important property that allows for the reconstruction of spectra using its inverse transform without losing any data. In order to work in the FD and restore the signal to its original form, CS-SCHT is therefore permitted (domain). The real basis of the various sequencies depicted in Fig. 1a is summarized in Fig. 1b. It has been proven through research that it has been used for spectrum estimations signal processing (Wu et al., 2012; Dur-e-Jabeen et al., 2017; Pei et al., 2014; Kyochi and Tanaka, 2014) and spectrum estimations (Aung et al., 2009). Fast N-point CS-SCHT is less efficient than the N-point DFT technique in terms of computational cost (Aung et al., 2009; 2008). This essay is divided into five pieces; section 2 discusses SD interpretation of phasor rotations. This paper is organized as section 1 is based on the introduction. Signal interpretation in SD is discussed in section 2. Section 3 derives the symmetry characteristics in SD with its effect. Section 4 explains and discusses the simulation results. Section 5 provides a synopsis of all conclusions.

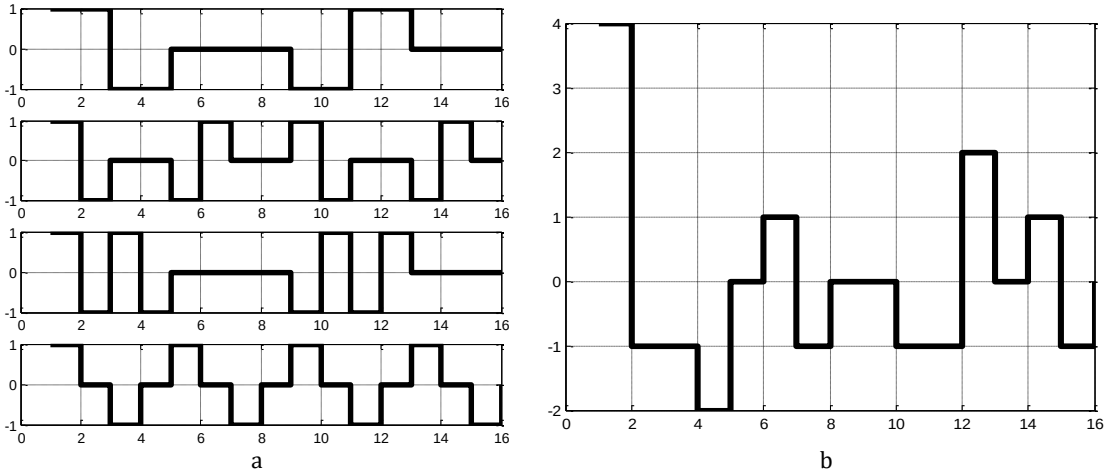

Fig. 1: a) Real part of row vectors with different sequency of CS-SCHT transform; b) Sum of four functions given in a

2. Perception and representation of complex input signals in sequency domain

The CS-SCHT transform along with its inverse CS-SCHT, is defined as in Aung et al. (2009),

$$\wp(\kappa) = \sum_{n=0}^{N-1} \aleph(n)\,(-1)^{\sum_{n_{r-0}}^{l-1} u}(-j)^{\sum_{n_r=0}^{l-1} v} \quad (1)$$

$$\aleph(n) = \frac{1}{N}\sum_{k=0}^{N-1} \wp(\kappa)\,(-1)^{\sum_{n_{r-0}}^{l-1} u}(j)^{\sum_{n_r=0}^{l-1} v} \quad (2)$$

where, $n = 0,1,2,\dots,N-1$, $\wp(k)$ is the sequency domain spectrum, the time domain symmetric signal is presented as $\aleph(n) = \left[\aleph\left(-\frac{M}{2}\right),\dots,\aleph(-1),\aleph(0),\dots,\aleph(\frac{N}{2}-1)\right]^t$, $k_g n = u$ and $k_f n = v$ are binary numbers. H_N is the N^{th} order of the CS-SCHT matrix and is represented below (Aung et al., 2009):

$$H_N = (-1)^{\sum_{n_r=0}^{l-1} u}(-j)^{\sum_{n_r=0}^{l-1} v} \quad (3)$$

Let $(-1) = e^{-j\pi}$ and $(-j) = e^{-j\pi/2}$ for easy analysis, therefore, suppose $\alpha = \sum_{n_r=0}^{l-1} u$ & $\beta = \sum_{n_r=0}^{l-1} v$, therefore Eq. 3 becomes:

$$H_N = e^{-j\pi\alpha} e^{-j(\frac{\pi}{2})\beta} \quad (4)$$

Transformed spectrum for any time domain signal such as, $\wp(k) = \Im\{\aleph(n)\}$, where; $\Im$ represents the transform and its time reversal is $\wp(-k) = \Im\{\aleph(-n)\}$. Therefore, for $\aleph(n) \Leftrightarrow \wp(k)$, $\aleph(n)$ and $\aleph(-n)$ are positive and negative sides of the time domain signal at the origin. $\wp(k)$ and $\wp(-k)$ are respective sequency domain spectra. These spectra have positive and negative sequencies with real and imaginary coefficients. Such complex value pairs are $\wp(k) = (Re(k) + jIm(k))$ and $\wp(-k) = (Re(-k) + jIm(-k))$. Each component is considered to define a rotation, positive for $\wp(k)$ counter-clockwise and negative $\wp(-k)$ for clockwise direction. In a fundamental sequency $(k = -1)$, the positive value completes one cycle around the origin with data points from $n = 0,1,2,\dots,N-1$ and starting position given by $\varphi^+ = tan^{-1}(Im(k)/Re(k))$ and similarly for the $(k = -1)$ phasor direction is clockwise with $\varphi^- = tan^{-1}(Im(-k)/Re(-k))$. The magnitude of each vector can be defined as $m^+ = \sqrt{Re\{k\}^2 + Im\{k\}^2}$ and $m^- = \sqrt{Re\{k-\}^2 + Im\{-k\}^2}$. The vector sum of both quantities is for the discrete increment in φ^+ and φ^- results in the final path around the origin.

The phase of the sequency component determines the starting angle around the origin and the sum of the sequency components provides the magnitude for each vector. For increasing the sequency values $(k = 2,3,4,..)$, the number of cycles is increased around the origin. For N-points data, 0^{th} and $(N/2)^{\text{th}}$ positions are arbitrary values (Aung et al., 2009). The other position values should be symmetric with respect to the suggested symmetry property. The relationship between time and transform domain is defined by phasor rotations with clockwise and counterclockwise directions that

make a circle, elliptical, or simple straight line motions in a complex plane for SD (McCabe et al., 2000; Dur-e-Jabeen and Monir, 2016). Fig. 2 shows that at different symmetries, the combination of positive and negative magnitudes and phasors, works along the complex plane. Many applications are investigated in the data analysis field employing symmetrical base (Rosell-Tarragó and Díaz-Guilera, 2021; Li et al., 2020; Qiao et al., 2022; Sreedharan et al., 2020), and these can be analyzed in the sequence domain utilizing transform domain.

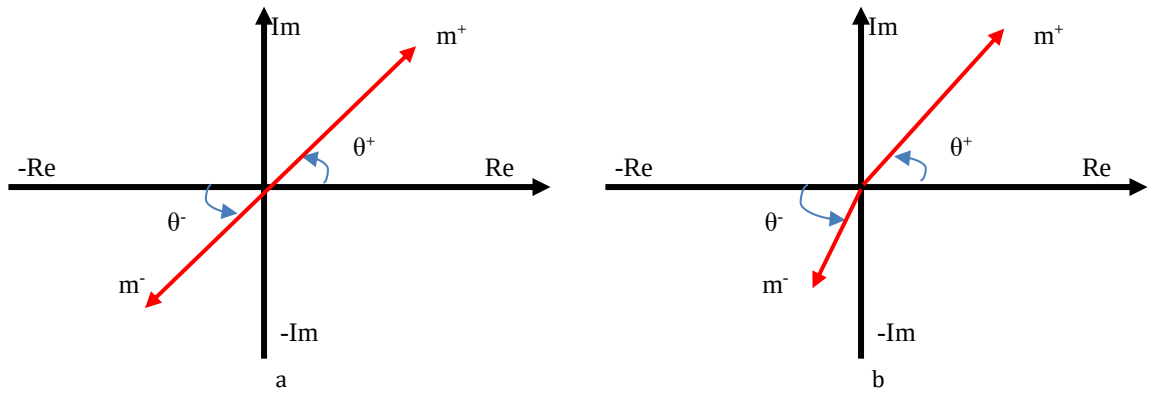

Fig. 2: a) Circular motion with complex values; b) Elliptical motion along the complex plane

3. Effects of symmetries

It's necessary to develop an understanding of how negative sequencies and complex numbers affect CHT's usual real-valued input. Consider one-dimensional CS-SCHT; as a result, the following is a representation of Eq. 1:

$$\wp(k) = \sum_{n=N/2}^{N/2-1}(\aleph(n) + j\aleph(n))e^{-j\pi\alpha}e^{-j(\pi/2)\beta} \quad (5)$$

By placing Euler identities, $e^{-j\pi\alpha} = cos(\pi\alpha) - jsin(\pi\alpha)$ and $e^{-j(\pi/2)\beta} = cos\left((\pi/2)\beta\right) - jsin\left((\pi/2)\beta\right)$ in Eq. 4, it becomes,

$$H_N = \begin{matrix} cos(\pi\alpha)cos\left((\pi/2)\beta\right) - jcos(\pi\alpha)\,sin\left((\pi/2)\beta\right) \\ -jsin(\pi\alpha)cos\left((\pi/2)\beta\right) + sin(\pi\alpha)\,sin\left((\pi/2)\beta\right) \end{matrix} \quad (6)$$

Eq. 6 is represented with trigonometric functions as below,

$$H_N = \begin{matrix} \frac{1}{2}\{cos(\pi\alpha + (\pi/2)\beta) + cos(\pi\alpha - (\pi/2)\beta)\} - \frac{j}{2}\{sin(\pi\alpha + (\pi/2)\beta) - sin(\pi\alpha - (\pi/2)\beta)\} \\ -\frac{j}{2}\{sin(\pi\alpha + (\pi/2)\beta) + sin(\pi\alpha - (\pi/2)\beta)\} + \frac{1}{2}\{cos(\pi\alpha - (\pi/2)\beta) - cos(\pi\alpha + (\pi/2)\beta)\} \end{matrix} \quad (7)$$

After simplification, H_N is given by,

$$H_N = cos(\pi\alpha - (\pi/2)\beta) - jsin(\pi\alpha + (\pi/2)\beta) \quad (8)$$

Now Eq. 5 becomes,

$$\wp(k) = \sum_{n=N/2}^{N/2-1}(\aleph_r(n) + j\aleph_i(n))\{cos(\pi\alpha - (\pi/2)\beta) - jsin(\pi\alpha + (\pi/2)\beta)\} \quad (9)$$

Hence, different combinations of Eq. 9 are presented below:

$\Rightarrow \aleph_R(n)cos(\pi\alpha - (\pi/2)\beta)$: Real Positive Even

$\Rightarrow j\aleph_I(n)cos(\pi\alpha - (\pi/2)\beta)$: Imaginary Positive Even

$\Rightarrow -\aleph_R(n)jsin(\pi\alpha + (\pi/2)\beta)$: Real Negative Odd

$\Rightarrow -j\aleph_I(n)jsin(\pi\alpha + (\pi/2)\beta)$: Imaginary Negative Odd

Therefore, by substituting these symmetries along with complex input $\aleph_R(n) + j\aleph_I(n)$ into Eq. 5, then obtain CS-SCHT as below for real and imaginary inputs:

$$\wp(k) = \sum_{n=0}^{N-1}\left(\aleph_R(n)cos(\pi\alpha - (\pi/2)\beta) + \aleph_I(n)sin(\pi\alpha + (\pi/2)\beta)\right) \quad (10)$$

$$\wp(k) = \sum_{n=0}^{N-1}\left(\aleph_R(n)sin(\pi\alpha - (\pi/2)\beta) - \aleph_I(n)cos(\pi\alpha + (\pi/2)\beta)\right) \quad (11)$$

Similarly, the inverse of CS-SCHT becomes,

$$\aleph_R(n) = \frac{1}{N}\sum_{k=0}^{N-1}\left(\wp_R(k)cos(\pi\alpha - (\pi/2)\beta) - \wp_I(n)sin(\pi\alpha + (\pi/2)\beta)\right) \quad (12)$$

$$\aleph_I(n) = \frac{1}{N}\sum_{k=0}^{N-1}\left(\wp_R(n)sin(\pi\alpha - (\pi/2)\beta) + \wp_I(n)cos(\pi\alpha + (\pi/2)\beta)\right) \quad (13)$$

Following are symmetries derived along with the respective signal structure.

A) Real value signal with even symmetry: If input $\aleph(n)$ is real and even symmetric; as $\aleph_{re}(n)$, that is,

$$\aleph(n) = \{\aleph(N-n)\ \};\quad 0 \le n \le (N-1) \tag{14}$$

Then Eq. 10 yields $\wp_I(k) = 0$. Hence CS-SCHT reduces to,

$$\wp_{re}(k) = \sum_{n=0}^{N-1}\left(\aleph_{re}(n)cos\left(\pi\alpha - (\pi/2)\beta\right)\right);\quad 0 \le k \le (N-1) \tag{15}$$

Which is itself a real value and even symmetric. Moreover, ICS-SCHT reduces to,

$$\aleph_{re}(n) = \frac{1}{N}\sum_{k=0}^{N-1}\left(\wp_{re}(k)cos\left(\pi\alpha + (\pi/2)\beta\right)\right);\quad 0 \le n \le (N-1) \tag{16}$$

B) Real value signal with odd symmetry: If input $\aleph(n)$ is real and odd symmetric; similar to $\aleph_{ro}(n)$, that is,

$$\aleph(n) = \{-\aleph(N-n)\ \};\quad 0 \le n \le (N-1) \tag{17}$$

then Eq. 11 yields $\wp_R(k) = 0$. Hence CS-SCHT reduces to,

$$\wp_{ie}(k) = -j\sum_{n=0}^{N-1}\left(\aleph_{ro}(n)sin\left(\pi\alpha + (\pi/2)\beta\right)\right);\quad 0 \le k \le (N-1) \tag{18}$$

It provides purely imaginary and odd symmetric, furthermore, $\wp_R(k) = 0$, so ICS-SCHT reduces to:

$$\aleph_{ro}(n) = \frac{j}{N}\sum_{k=0}^{N-1}\left(\wp_{ie}(k)sin\left(\pi\alpha - (\pi/2)\beta\right)\right);\quad 0 \le n \le (N-1) \tag{19}$$

C) Imaginary value signal with even symmetry: If input $j\aleph(n)$ is imaginary and even symmetric; as $\aleph_{ie}(n)$, then Eq. 5 yields $\wp_R(k) = 0$. Hence CS-SCHT reduces to,

$$\wp_{ie}(k) = \sum_{n=0}^{N-1}\left(\aleph_{ie}(n)cos\left(\pi\alpha - (\pi/2)\beta\right)\right);\quad 0 \le k \le (N-1) \tag{20}$$

It is observed that the spectrum has imaginary value and even symmetric $\wp_{ie}(k)$, so ICS-SCHT becomes,

$$\aleph_{ie}(n) = \frac{1}{N}\sum_{k=0}^{N-1}\left(\wp_{ie}(k)cos\left(\pi\alpha - (\pi/2)\beta\right)\right);\quad 0 \le n \le (N-1) \tag{21}$$

D) Imaginary value signal with odd symmetry: If input $j\aleph(n)$ is imaginary and odd symmetric; as $\aleph_{io}(n)$, then Eq. 5 yields $\wp_R(k) = 0$. Hence CS-SCHT reduces to,

$$\wp_{ro}(k) = -j\sum_{n=0}^{N-1}\left(\aleph_{io}(n)sin\left(\pi\alpha - (\pi/2)\beta\right)\right);\quad 0 \le k \le (N-1) \tag{22}$$

It is observed that the spectrum has imaginary value and even symmetric $\wp_{ie}(k)$, and ICS-SCHT reduces to,

$$\aleph_{io}(n) = \frac{j}{N}\sum_{k=0}^{N-1}\left(\wp_{ro}(k)sin\left(\pi\alpha - (\pi/2)\beta\right)\right);\quad 0 \le n \le (N-1) \tag{23}$$

E) Complex value signal with even symmetry: If input $\aleph(n) + j\aleph(n)$ is complex and even symmetric; as $\aleph_{ce}(n)$, then Eq. 5 yields $\wp_I(k) = 0$. Hence CS-SCHT reduces to,

$$\wp_{ce}(k) = \sum_{n=0}^{N-1}\left(\aleph_{ce}(n)cos\left(\pi\alpha - (\pi/2)\beta\right)\right);\quad 0 \le k \le (N-1) \tag{24}$$

$$\aleph_{ce}(n) = \frac{1}{N}\sum_{k=0}^{N-1}\left(\wp_{ce}(k)cos\left(\pi\alpha - (\pi/2)\beta\right)\right);\quad 0 \le n \le (N-1) \tag{25}$$

F) Complex value signal with odd symmetry: If input $\aleph(n) + j\aleph(n)$ is complex and odd symmetric; as $\aleph_{co}(n)$, then Eq. 5 yields $\wp_R(k) = 0$. Hence CS-SCHT reduces to:

$$\wp_{co}(k) = \sum_{n=0}^{N-1}\left(\aleph_{co}(n)cos\left(\pi\alpha + (\pi/2)\beta\right)\right);\quad 0 \le k \le (N-1) \tag{26}$$

which is complex and odd-symmetric. Moreover, ICS-SCHT reduces to:

$$\aleph_{co}(n) = \frac{1}{N}\sum_{k=0}^{N-1}\left(\wp_{co}(k)sin\left(\pi\alpha - (\pi/2)\beta\right)\right);\quad 0 \le n \le (N-1) \tag{27}$$

The generalization of real input CS-SCHT is the interpretation of the sequence domain representation of complex input CS-SCHT. The spectrum contains both "even symmetric real output components" and "odd symmetric imaginary output components" because the real inputs with no symmetry lead to Hermitian symmetry.

4. Results and discussion

Symmetry properties, such as $\aleph_{re}(n)$, which provides $\wp_{re}(k)$, which is the sum of the final result on the complex plane, determined in the previous section. Table 1 shows the symmetry characteristics of the sequency domain. Table 1 displays the signal's characteristics in the time domain as well as the frequency and sequency domain.

It demonstrates that an even spectrum is seen for input signals that are complex, fictitious, and real alike. However, when the input signal lacks symmetry for real or imaginary signals, respectively, the Hermitian and anti-Hermitian spectra are obtained.

4.1. 1D signal processing application

An actual signal with even symmetry is shown in Fig. 3a, along with a CS-SCHT representation of its sequency. There are only symmetrical real components in the spectrum. The spectrum's phasor representation is shown in Fig. 3b. Adding these

phasors causes the real axis to move in a straight line. A peculiarly symmetric real signal and its sequency spectrum are shown in Fig. 4a. Only odd symmetric imaginary values are present in the spectrum. The spectrum's phasor representation is shown in Fig. 4b, where it is clear that the addition of a phasor will cause it to move in a straight line along the imaginary axis. An actual signal without symmetry and its sequency spectrum are shown in Fig. 5a. Even symmetric real and odd symmetric imaginary components make up the spectrum. In Fig. 5b, the phasor representation of the sequency spectrum, it is clear that adding the phasor would cause a straight-line motion down the real axis.

An imaginary signal with equal symmetry and its sequency spectrum are shown in Fig. 6a. The components of the spectrum are imaginary, even-symmetrical parts. In Fig. 6b, the sequency spectrum is shown as a phasor, and it is obvious that adding the phasor would cause a straight-line motion along the imaginary axis. Fig. 7a shows an imaginary signal with an odd symmetry and its sequency spectrum. Odd symmetric real components make up the spectrum. Fig. 7b shows how the sequency spectrum is represented as a phasor. It should be clear that the addition of a phasor would cause a motion in a straight line along the real axis.

A hypothetical or imaginary signal without symmetry and its sequency spectrum are shown in Fig. 8a. Odd symmetric real and even symmetric imaginary components make up the spectrum. Fig. 8b shows the sequency spectrum's phasor representation. Fig. 8b makes it clear that the addition of the phasor would cause a straight-line motion along the hypothetical axis. It is simple to demonstrate that all fictitious components will cancel out due to hermitian symmetry, leaving just real coefficients with no symmetry. The hermitian signal has only real components and no symmetric imaginary components in its sequency spectrum, and even symmetric real values Likewise, anti-hermitian is the opposite.

Table 1: Comparison of symmetry properties of DFT and CS-SCHT (Dur-e-Jabeen and Monir, 2016)

Signal time domain property	Frequency domain property for DFT	Sequency domain property for CS-SCHT
Real and even	Real and even	Real and even
Imaginary and even	Imaginary and even	Imaginary and even
Complex and even	Complex and even	Complex and even
Real and odd	Imaginary and odd	Imaginary and odd
Imaginary and odd	Real and odd	Real and odd
Complex and odd	Complex and odd	Complex and odd
Real and no symmetry	Hermitian	Hermitian
Imaginary and no symmetry	Anti-Hermitian	Anti-Hermitian
Complex and no symmetry	Complex and no symmetry	Complex and no symmetry
Hermitian	Real and no symmetry	Real and no symmetry
Anti-Hermitian	Imaginary and no symmetry	Imaginary and no symmetry

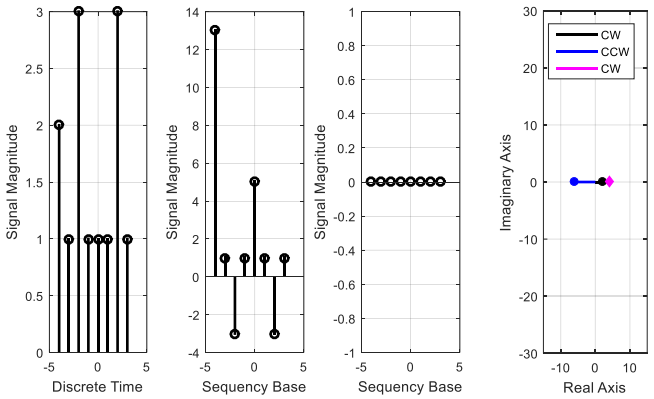

a b

Fig. 3: a) Even-real valued signal and symmetric spectrum, b) Respective phasor illustration

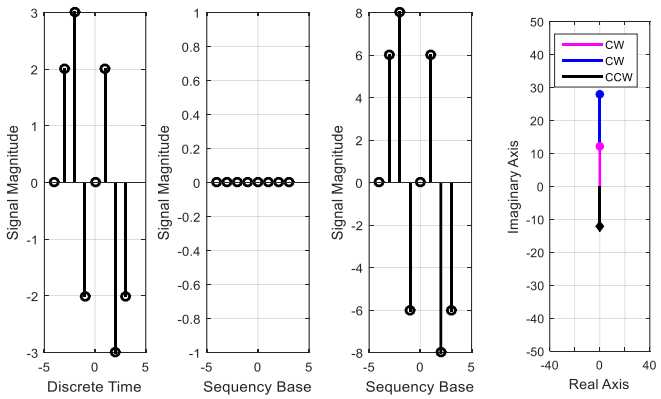

a b

Fig. 4: a) Odd-real valued signal and odd-symmetric spectrum, b) Respective phasor illustration

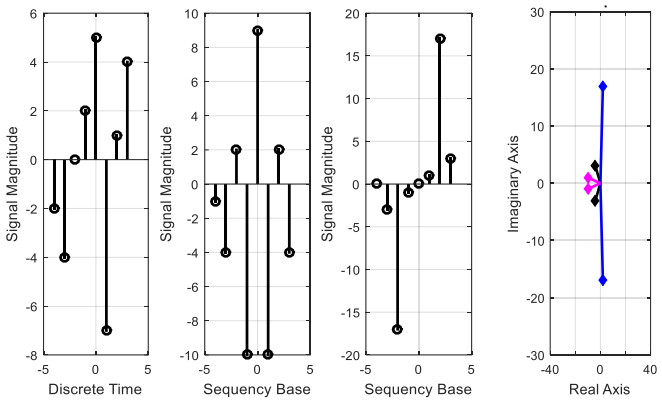

a b

Fig. 5: a) Non-symmetric real value signal and non-symmetric spectrum, b) Respective phasor illustration

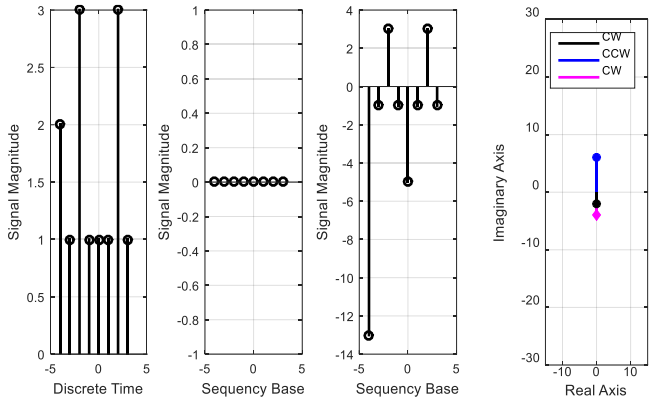

a b

Fig. 6: a) Even-imaginary valued signal and even symmetric spectrum, b) Phasor illustration

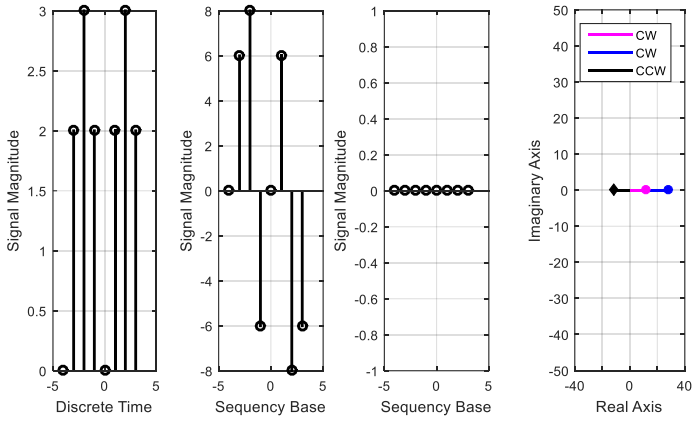

a b

Fig. 7: a) Odd symmetry-imaginary valued signal and spectrum, b) Respective phasor diagram

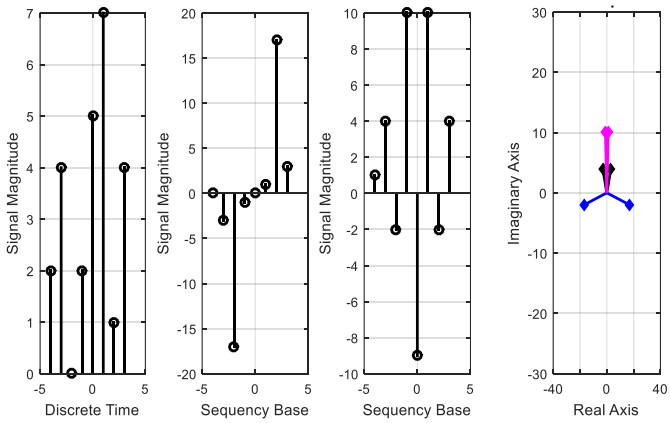

a b

Fig. 8: a) Imaginary valued signal and non-symmetric spectrum, b) Phasor diagram for imaginary value signal and no symmetry

4.2. 2D image processing application

Either the spatial domain or the transform domain can be used for digital image processing. Symmetry qualities play a significant role in signal and image processing. CS-SCHT is applied to the binary, gray, and color images to analyze the performance of the sequency domain symmetry properties. That explains how the combination of positive and negative sequency phasors causes motion along the real and hypothetical/imaginary axis. Specifically, how the magnitude and phasor response present its behavior in the sequency domain on a complex plane.

Figs. 9-12, show the symmetrical image with different resolutions such as 96x96, 256x256, 296x296, and 512x512. Magnitude and phase response are presented along with the respective images, and all image sequency spectra are FFT-shifted.

The shape of the relevant image is revealed by the magnitude response, while the boundary lines are shown by the phase response, allowing us to recognize the image in its original spatial context.

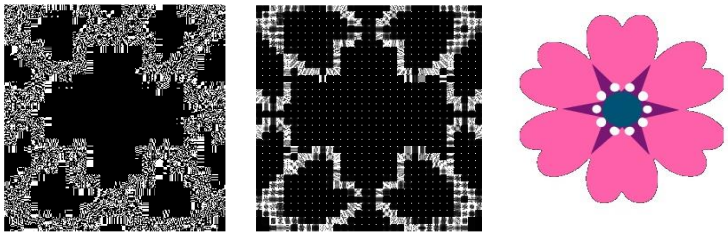

a b c

Fig. 9: a) Symmetric color image, b) Magnitude spectrum, c) Phase spectrum

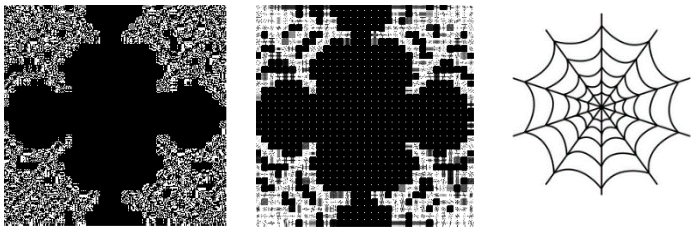

a b c

Fig. 10: a) Symmetric binary image, b) Magnitude spectrum, c) Phase spectrum

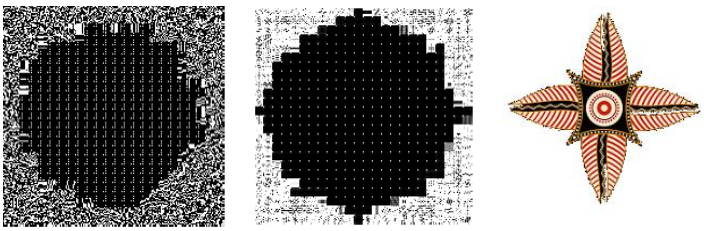

a b c

Fig. 11: a) Symmetric color image, b) Magnitude spectrum, c) Phase spectrum

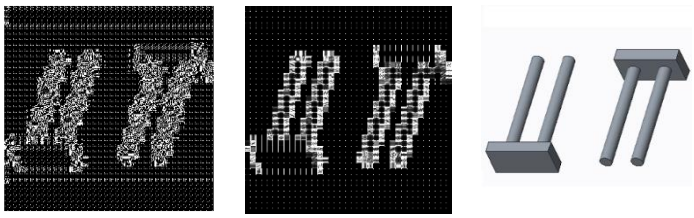

a b c

Fig. 12: a) Anti-symmetric image, b) Magnitude spectrum, c) Phase spectrum

5. Conclusion

In this study, phasor rotations in the sequency domain are also computed along with the symmetry features of CS-SCHT. The sequency spectrum of a complex input without symmetry is demonstrated in this study to be complex without symmetry as well. Therefore, there is no correlation between the positive and negative sequency coefficients. However, the subsequent trajectory that was tracked through the complex plane can still be given to us using the phasor representation. The magnitude and phase values of the two phasors can differ when the input is complex and non-symmetric. When the sole difference is in the phase value, the resulting path will depict a straight-line motion. The combination of two component phasors will yield the motion's angle. Symmetry properties play and very significant role in the number of biomedical, methodical, and digital signal processing applications. Because the transform domain reduces the computational cost in terms of the half spectral coefficients, it can be

employed for image analysis with deep learning algorithms alongside the sequency domain to get similar results as the frequency domain by using DFT. Transform can be utilized for the extraction and analyze various aspects and characteristics of medical images considering the different input signals.

Compliance with ethical standards

Conflict of interest

The author(s) declared no potential conflicts of interest with respect to the research, authorship, and/or publication of this article.

References

Asli BHS and Flusser J (2017). New discrete orthogonal moments for signal analysis. Signal Processing, 141: 57-73. https://doi.org/10.1016/j.sigpro.2017.05.023

Aung A (2009). Sequency-ordered complex Hadamard transforms and their applications to communications and signal processing. Ph.D. Dissertation, Nanyang Technological University, Singapore, Singapore.

Aung A, Ng BP, and Rahardja S (2008). Sequency-ordered complex Hadamard transform: Properties, computational complexity and applications. IEEE Transactions on Signal Processing, 56(8): 3562-3571. https://doi.org/10.1109/TSP.2008.923195

Aung A, Ng BP, and Rahardja S (2009). Conjugate symmetric sequency-ordered complex Hadamard transform. IEEE Transactions on Signal Processing, 57(7): 2582-2593. https://doi.org/10.1109/TSP.2009.2017572

Bahrami S and Naderi M (2014). Encryption of video main frames in the field of DCT transform using A5/1 and W7 stream encryption algorithms. Arabian Journal for Science and Engineering, 39(5): 4077-4088. https://doi.org/10.1007/s13369-014-1077-8

Dur-e-Jabeen and Monir G (2016). Two-dimensional spatiochromatic signal processing using concept of phasors in sequency domain. Electronics Letters, 52(11): 968-970. https://doi.org/10.1049/el.2016.0059

Dur-e-Jabeen, Kumar K, Haseeb A, and Faizan M (2017). Spectral analysis of chirp and sinusoidal signals in complex domain. In the 10th International Conference on Electrical and Electronics Engineering, IEEE, Bursa, Turkey: 1137-1140.

Dur-e-Jabeen, Monir G, and Azim F (2016). Sequency domain signal processing using complex Hadamard transform. Circuits, Systems, and Signal Processing, 35(5): 1783-1793. https://doi.org/10.1007/s00034-015-0138-x

Kyochi S and Tanaka Y (2014). General factorization of conjugate-symmetric Hadamard transforms. IEEE Transactions on Signal Processing, 62(13): 3379-3392. https://doi.org/10.1109/TSP.2014.2326620

Li X, Hu G, Zhu J, Zuo W, Wang M, and Zhang L (2020). Learning symmetry consistent deep CNNs for face completion. IEEE Transactions on Image Processing, 29: 7641-7655. https://doi.org/10.1109/TIP.2020.3005241

Mahmmod BM, Ramli ARB, Abdulhussain SH, Al-Haddad SAR, and Jassim WA (2018). Signal compression and enhancement using a new orthogonal-polynomial-based discrete transform. IET Signal Processing, 12(1): 129-142. https://doi.org/10.1049/iet-spr.2016.0449

McCabe A, Caelli T, West G, and Reeves A (2000). Theory of spatiochromatic image encoding and feature extraction. Journal of the Optical Society of America A, 17(10): 1744-1754. https://doi.org/10.1364/JOSAA.17.001744 **PMid:11028522**

Pei SC, Wen CC, and Ding JJ (2014). Conjugate symmetric discrete orthogonal transform. IEEE Transactions on Circuits and Systems II: Express Briefs, 61(4): 284-288. https://doi.org/10.1109/TCSII.2014.2305011

Proakis JG (2007). Digital signal processing: Principles, algorithms, and applications. 4th Edition, Pearson Education India, Delhi, India.

Qiao YL, Gao L, Liu SZ, Liu L, Lai YK, and Chen X (2022). Learning-based intrinsic reflectional symmetry detection. IEEE Transactions on Visualization and Computer Graphics. https://doi.org/10.1109/TVCG.2022.3172361 **PMid:35522628**

Rahardja S and Falkowski BJ (1999). Family of unified complex Hadamard transforms. IEEE Transactions on Circuits and Systems II: Analog and Digital Signal Processing, 46(8): 1094-1100. https://doi.org/10.1109/82.782059

Rehman MU and Mehmood A (2018). Approximating structured singular values for discrete Fourier transformation matrices. International Journal of Advanced and Applied Sciences, 5(12): 119-125. https://doi.org/10.21833/ijaas.2018.12.014

Rosell-Tarragó G and Díaz-Guilera A (2021). Quasi-symmetries in complex networks: A dynamical model approach. Journal of Complex Networks, 9(3): cnab025. https://doi.org/10.1093/comnet/cnab025

Shukla D and Sharma M (2018). A new approach for scene-based digital video watermarking using discrete wavelet transforms. International Journal of Advanced and Applied Sciences, 5(2): 148-160. https://doi.org/10.21833/ijaas.2018.02.022

Sreedharan JK, Turowski K, and Szpankowski W (2020). Revisiting parameter estimation in biological networks: Influence of symmetries. IEEE/ACM Transactions on Computational Biology and Bioinformatics, 18(3): 836-849. https://doi.org/10.1109/TCBB.2020.2980260 **PMid:32175871 PMCid:PMC8555700**

Tian C, Zhang Q, Sun G, Song Z, and Li S (2018). FFT consolidated sparse and collaborative representation for image classification. Arabian Journal for Science and Engineering, 43(2): 741-758. https://doi.org/10.1007/s13369-017-2696-7

Usman SM, Latif S, and Beg A (2020). Principle components analysis for seizures prediction using wavelet transform. International Journal of Advanced and Applied Sciences, 6(3): 50-55. https://doi.org/10.21833/ijaas.2019.03.008

Wu J, Wang L, Yang G, Senhadji L, Luo L, and Shu H (2012). Sliding conjugate symmetric sequency-ordered complex Hadamard transform: Fast algorithm and applications. IEEE Transactions on Circuits and Systems I: Regular Papers, 59(6): 1321-1334. https://doi.org/10.1109/TCSI.2011.2173386